Dyes and Pigments 170 (2019) 107604

Contents lists available at ScienceDirect

Dyes and Pigments

journal homepage: www.elsevier.com/locate/dyepig

On the design of new europium heteroaromatic carboxylates for OLED application☆

Daniil S. Koshelev[a,*], Tatyana Yu Chikineva[a], Vladislava Yu Kozhevnikova (Khudoleeva)[a], Alexey V. Medvedko[b], Andrey A. Vashchenko[c], Alexander S. Goloveshkin[d], Dmitry M. Tsymbarenko[b], Alexey A. Averin[e], Anna Meschkov[f,g], Ute Schepers[f,g], Sergey Z. Vatsadze[b], Valentina V. Utochnikova[a,b]

[a] Faculty of Materials Science, M.V. Lomonosov Moscow State University, 1/73 Leninskye Gory, Moscow, 119991, Russia
[b] Department of Chemistry, M.V. Lomonosov Moscow State University, 1/3 Leninskye Gory, Moscow, 119991, Russia
[c] P.N. Lebedev Physical Institute, Leninsky Prosp. 53, Moscow, 119992, Russia
[d] A. N. Nesmeyanov Institute of Organoelement Compounds, Vavilova Str., 28, Moscow, 117312, Russia
[e] A. N. Frumkin Institute of Physical Chemistry and Electrochemistry, Leninsky Prosp. 31/5 P.2, Moscow, 119071, Russia
[f] Institute of Functional Interfaces, Karlsruhe Institute of Technology, Karlsruhe, Germany
[g] Institute of Organic Chemistry, Karlsruhe Institute of Technology, Karlsruhe, Germany

ARTICLE INFO

Keywords:
Luminescence
Lanthanides
Carboxylates
OLED
Benzoxazole
Benzothiazole

ABSTRACT

The approach to the directed synthesis of lanthanide aromatic carboxylates – precursors to the electroluminescent materials, - was proposed, namely the conjugation length increase and heteroatom introduction in the appropriate position in combination with the neutral ligand introduction. This resulted in the isolation of a series of new lanthanide complexes, among which the highest electroluminescence efficiency was obtained for mixed-ligand europium benzothiazole-2-carboxylate with bathophenanthroline in a solution-processed OLED. The peculiarities of energy transfer processes allowed obtaining luminescence thermometer materials based on this system, which demontrated the sensitivity of 2.8%/K in the physiological range.

1. Introduction

Luminescent lanthanide (III) coordination compounds (CC) are unique candidates for electroluminescent materials as they offer ultimate colour saturation due to their narrow luminescence bands. They also have potential for a high internal quantum efficiency of electroluminescence because they are capable of harvesting triplet excitons for light emission [1], so they have attracted considerable interest as OLED emission layer (EML) materials [2–8]. The mostly utilized technique of OLED processing is vacuum deposition, as it ensures high efficiency. However, volatility is required of luminescent materials in that case; besides, thermal evaporation is cost-ineffective and provides lower resolution than solution process [3,9,10]. In contrast, solution deposition of the emitting layers requires only solubility. In addition, this technique offers a whole number of variations, i.e. slot-die coating, blade coating, ink-jet printing, roll-to-roll process [11–15] and enables the obtaining of OLEDs of any size. But the most critical problem of solution-processed devices is orders of magnitude lower efficiency. So, even europium mixed-ligand (ML) aromatic carboxylates, among which is the one with the record photoluminescence quantum yield (PLQY) value [16], demonstrated electroluminescence with the efficiency of only up to 25 Cd/m^2 that is too low even in comparison to europium volatile complexes, such as β-diketones (i.e. 400 Cd/m^2 for europium dibenzoylmethanate with phenanthroline [17] or 72 Cd/m^2 for recently reported europium pyrazole-substituted β-diketone with batophenanthroline [18]. Still solution processing is promising in manufacturing and material cost decreasing, which requires simultaneous solution of two tasks: the search of the new materials and the development of the solution procession of OLEDs. The present work is aimed to give impact to the first one.

Thus, design of the luminescent material precursors based on lanthanide CCs must be started from the ligand design instead of the undirected synthesis. We selected aromatic carboxylates for the investigation, as they ensure high chemical stability and the high PLQY values of lanthanide CCs [19–28]. Their crucial issues usually are low solubility, particularly in water, due to the tendency to polymerize

☆ Electronic Supplementary Information (ESI) available.

* Corresponding author.
E-mail address: valentina@inorg.chem.msu.ru (D.S. Koshelev).

https://doi.org/10.1016/j.dyepig.2019.107604
Received 12 April 2019; Received in revised form 30 May 2019; Accepted 30 May 2019
Available online 31 May 2019
0143-7208/ © 2019 Elsevier Ltd. All rights reserved.

[22,29–33] and low charge carrier mobility [20,34–36]. Thus, the ligand design was aimed on the increase of the complex solubility and mobility, as well as absorption. The goal of the work was to verify the prospectiveness of such a material design for obtaining of the materials for potential use in bioimaging and OLEDs. In the present work their solution-processed OLED performance was demonstrated in particular.

There are several methods to increase the solubility, including in water for bioimaging and in organic solvents for solution-processable OLED. However, even though there is a large amount of experimental data that allows scientists to selectively modify the properties of the complexes (for example, solubility and luminescence intensity) unpredictable results still occur. So, the ML complex formation may result in both solubility increase [37–40] or decrease [16,41,42]. The introduction of the aliphatic chain into the ligand usually increases solubility [43–46] but decreases the luminescence quantum yield due to the quenching, originating from the CH-vibrations [44,47–50]. Ligand fluorination helps avoiding the latter problem, but leads to the decrease of the ligand molar absorption coefficient and complex stability in solution [24,51–54]. The introduction of a heteroatom (for instance N) into the α-position relative to a carboxylic group of the ligand was recently shown as another efficient approach, still lacking the listed drawbacks [55]. It will be used in the present work.

Important is that the heteroatom introduction (not only N but also S,O) was also shown to increase electron mobility, particularly of the highly conjugated compounds [56]. It also helps increasing the triplet state energy (i.e. benzoate (24800 cm^{-1}) [57] *vs* picolinate (25773 cm^{-1}) [58] or even 2-furanoate (29200 cm^{-1}) [58]). In order to achieve high sensitization efficiency of lanthanide luminescence, ligands triplet state energy should be above lanthanides excited state energy, and the optimal difference is usually believed to make up about 2500–4000 cm^{-1} [59]. So, for instance, europium excited state ($^5D_0$ (Eu^{3+}) = 17200 cm^{-1}) requires triplet state energy over 20000 cm^{-1}, while for terbium ($^5D_4$ (Tb^{3+}) = 20500 cm^{-1}) the triplet state energy over 23000 cm^{-1} is preferential, though there are some exceptions [60].

Increasing of conjugation length, that is the number of conjugated double bonds, can also increase ligand molar absorption coefficient [61–65]. At the same time, it results in decrease of the triplet excited state energy [61], which can lead to the decrease of sensitization efficiency; but as mentioned above, the heteroatom introduction can help avoiding this problem. There are many studies concerning coordination compounds based on monocyclic benzoic [24,66–68] and picolinic [43,58,69] acids derivates as well as on bicyclic acids derivates (naphthoic [70], benzofuran carboxylic [71,72], quinoline carboxylic acid [73–76]). But basing on the mentioned above dependence it can be suggested new forms of perspective ligands.

So, in order to combine high solubility, high absorption and charge carrier mobility, conjugated heteroaromatic carboxylate ligands were used in the present work, namely benzoxazole-2-carboxylate $(boz)^-$ and benzothiazole-2-carboxylate $(btz)^-$ were obtained, and the role of the second heteroatom (O or S) was studied (Fig. 1). Lanthanide homo- and mixed-ligand carboxylates with these ligands and neutral *o*-phenanthroline (Phen) and bathophenanthroline (BPhen) ligands were obtained and studied as precursors to OLED emitting layer materials [27,77–79].

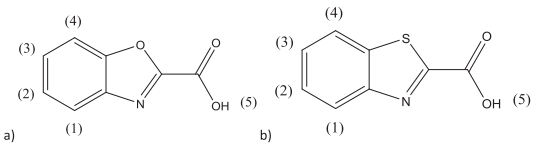

Fig. 1. a) Benzoxazole-2-carboxylic acid (H(boz)) b) benzothiazole-2-carboxylic acid (H(btz)). Positions of H atoms are enumerated for signals in ^1H NMR spectra assignment.

2. Experimental section

2.1. Materials and methods

All solvents, including deuterated solvents (D_2O, DMSO-d_6), and chemicals were purchased from commercial sources.

2.2. Aniline and 2-aminophenol were purchased from SigmaAldrich

Lanthanide salts were purchased from Huizhou GL Technology Co.

All other chemicals were purchased from Component-Reactive. Deuterated solvents were purchased from Carl Roth Gmbh.

^1H, ^{13}C NMR spectra were recorded at 25 °C using Agilent 400 MR spectrometer with the operating frequency of 400 and 100 MHz respectively. Chemical shifts are reported in ppm relative to residual solvent signals. **Elemental analysis** was performed on the microanalytical device Heraeus Vario Elementar. **Thermal analyses** were carried out on a thermoanalyzer STA 409 PC Luxx (NETZSCH, Germany) in the temperature range of 20–1000 °C in argon atmosphere, heating rate 10°/min. The composition of formed gases was determined by quadrupole mass spectrometer QMS 403C Aëolos (NETZSCH, Germany), combined by thermoanalizer NETZSCH STA 409 PC Luxx. Mass spectra were recorded for mass numbers 18 (H_2O), 44 (CO_2) и 58 ($CH_3C(O)CH_3$).

IR spectra in the ATR mode were recorded on a spectrometer SpectrumOne (PerkinElmer) in the region of 400–4000 cm-1.

X-ray powder diffraction (XRD) measurements were performed on a Bruker D8 Advance Vario diffractometer with LynxEye detector and Ge (111) monochromator, λ(CuKα$_1$) = 1.54060 Å, θ/2θ scan from 6.0° to 60°, step size 0.02°, in transmission mode, with the sample deposited between Mular films.

Single crystal X-ray diffraction (SC-XRD) studies were carried out on a Bruker APEX-II CCD diffractometer. The crystal was kept at 120 K during data collection. Using Olex2 [80], the structure was solved with the olex2.solve [81] structure solution program using Charge Flipping and refined with the XL [82] refinement package using Least Squares minimisation.

The solubility of the CC lanthanides was measured at room temperature according to the following procedure: a suspension of 150 mg of each compound in 10 mL of solvent was refluxed for 1 h and thereafter cooled to room temperature. Then 5 mL of the solution were filtered into a cup with known mass, the solvent was evaporated. and the change of the cup's mass corresponded to the amount of the dissolved product.

Absorption spectra were recorded in the region 250–800 nm with a Perkin–Elmer Lambda 650 spectrometer. **Emission spectra** was measured with a Fluorolog 3 spectrofluorometer over excitation with a xenon lamp. For the determination of the **photoluminescence quantum yields in solid state**, an integration sphere Quanta Phi was used. **Luminescence lifetime** measurements were recorded and detected on the same system. Lifetimes are averages of at least three independent measurements. All luminescence decays proved to be perfect single-exponential functions. **Photoluminescence spectra** at two temperatures (77, 298 K) were obtained on a S2000 (Ocean Optics) multichannel spectrometer with excitation by LGI-21 nitrogen laser (λ_{ex} = 337 nm). Thermal dependence of luminescence properties was measured on the same device using thermal control device and heating element. **Electroluminescence spectra** were measured on a PicoQuant time-correlated single photon counting system used as a conventional spectrofluorimeter. Spectral resolution was 4 nm. Electroluminescence intensity was normalized by integration time, which allows comparing different spectra.

OLED manufacturing took place in a clean room class 10000 (Lebedev Physical Institute, Moscow, Russia) in a glove-box under an argon atmosphere. The substrates were cleaned by ultrasonication in the following media: NaOH aqueous solution, distilled water, acetone

and 2-propanol for 16 min each. A 40 nm-thick poly(3,4-ethylenedioxythiophene):poly(styre-nesulfonate) (PEDOT:PSS) hole-injective layer was first deposited. An aqueous solution of PEDOT:PSS (5 mL) was poured onto the preheated (70 °C) patterned ITO glass substrate, after which the substrate was rotated for 60 s at 2000 rpm. Finally, the deposited film was annealed in air at 80 °C for 60 min. As a hole-transport layer (20 nm) poly-TPD solution was spin-coated from chlorobenzene (c = 5 gL^{-1}) and was annealed in argon at 220 °C for 30 min. The emission layer was spin-coated from the solution (c = 5 gL^{-1}) on the heterostucture or on the glass substrate. The ~15 nm-thick electron-transport/hole-blocking layer (TPBi) was thermally evaporated (Univex-300, LeybordHeraeus) followed by a ~1 nm-thick LiF layer and a > 100 nm-thick aluminium layer as the cathode under a pressure below 10^{-6} mm Hg. The thickness of the layers was controlled by using a quartz indicator. The contacts were attached to the electrodes, and the device was sealed with epoxy resin (Norland Optical Adhesive).

Quantum chemical calculations. The geometry of the ground state of the K(carb) and Eu(carb)$_3$ molecules was optimized using Firefly 8.2 package [83] in a framework of the DFT theory with PBE0 functional, full electron basis set 6-31G(d, p) for C, N, O, S and H atoms, and quasi-relativistic Stuttgart-Koeln ECP52MWB pseudopotential (f-electrons in core) with appropriate basis set for Eu atom [84].

For each molecule all relevant structural isomers were considered, optimized and the lowest-energy isomer was chosen for further calculations. The optimized molecular geometries were checked for the absence of imaginary frequencies in the vibrational spectra.

TD-DFT calculations were performed at the same PBE0/6-31G(d, p) + ECP52MWB level for the optimized geometry of molecules, 20 singlet single excited states were considered. The energies of the frontier orbitals were calculated using the DFT and TDDFT results. The energy of the HOMO was obtained as the eigenvalue of DFT calculation for the ground state, while the energy of the LUMO was computed as E (HOMO) + Eg, where Eg is the lowest vertical transition energy in TD-DFT specturm. The details of this approach were reported in Ref. [39].

2.3. Synthesis

2.3.1. Synthesis of K(boz)

Methyl benzoxazole-2-carboxylate. A mixture of 2-aminophenol (2.11 g, 19.4 mmol) and methyl 2,2,2-trimethoxyacetate (10.17 g, 62.0 mmol) were flushed with argon and stirred at 100 °C for 42 h. Excess of methyl 2,2,2-trimethoxyacetate was distilled off under reduced pressure. The residue was suspended in diethyl ether (100.0 mL), filtered, and obtained powder was washed with diethyl ether until discoloration of filtrate. The beige powder was purified with column chromatography (silica gel, particle size 40–63 μm) eluting with petroleum ether – ethyl acetate 3:1. R_f (PE:EA 3:1) 0.28. Yield 1.04 g (31%). Light yellow powder.

^{1}H NMR (400 MHz, $CDCl_3$) δ (ppm): 7.90 (d, J = 8 Hz, 1H), 7.68 (d, J = 8 Hz, 1H), 7.51 (t, J = 8 Hz, 2H), 4.10 (s, 3H). ^{13}C NMR (100 MHz, $CDCl_3$) δ (ppm): 156.89, 152.49, 150.87, 140.45, 128.24, 125.83. NMR spectra coincide with the literature data [85].

Potassium benzoxazole-2-carboxylate was obtained according to Scheme 1. 0.87 M aq. KOH (6.06 mL) were added to the solution methyl-benzoxazole-2-carboxylate (0.93 g, 5.3 mmol) in THF (10.5 mL). Orange solution was stirred at rt for 1 h and solvent removed completely. Yield 1.04 g (98%). Beige solid. Mp. 307–310 °C (dec.). $C_8H_5NO_3$: HRMS, *m/z*: calcd. for $[M - H]^-$, 162.0197; found, 162.0189. IR-ATR (KBr, cm^{-1}): 3279, 1652, 1542, 1389, 1330, 1255, 1161, 843, 738.^{1}H NMR (400 MHz, D_2O) δ (ppm): 7.69 (d, J = 8 Hz, 1H), 7.65 (d, J = 8 Hz, 1H), 7.37 (t, J = 8 Hz, 1H), 7.32 (t, J = 8 Hz, 1H). ^{13}C NMR (100 MHz, D_2O) δ (ppm): 161.66, 157.92, 149.93, 139.32, 127.01, 125.11, 120.26, 111.40. Calcd: C, 58.90; H, 3.09; N, 8.59%; found: C, 59.02; H, 2.98; N, 8.60%.

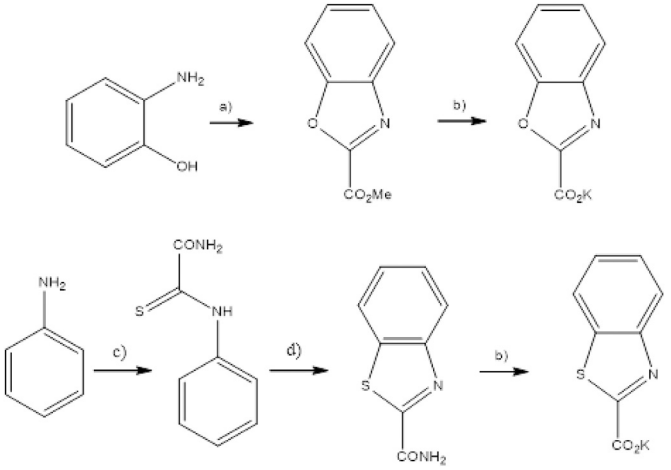

Scheme 1. Synthesis of K(boz) and K(btz). a) $(MeO)_3CCO_2Me$, 100 °C, 42 h. b) KOH, THF, H_2O, rt. c) 2-chloroacetamide, S, DMF, Et_3N, rt. d) $K_3Fe(CN)_6$, NaOH, H_2O, reflux.

2.3.2. Synthesis of K(btz)

2-(Phenylamino)-2-thiooxoacetamide. The freshly distilled aniline (3.82 g, 40.5 mmol) were dissolved in dry DMF (37 mL). To prepared solution of trimethylamine (7.4 mL) and sulfur (5.14 g, 161.1 mmol) were sequentially added under vigorous stirring. The light brown solution was stirred for 30 min and then chloroacetamide (3.43 g, 36.7 mmol) was added. The resulted red solution was stirred for 14 h at room temperature and diluted with water (440 mL). The sulfur was removed by filtration and washed with acetone until discoloration of filtrate. Solvents from filtrate were removed and the residue was recrystallized from ethanol. Yield 3.06 g (46%). Orange needles. ^{1}H NMR (400 MHz, DMSO-d_6) δ (ppm): 12.10 (s, 1H), 8.14 (d, J = 16 Hz, 2H), 7.92 (d, J = 8 Hz, 2H), 7.42 (t, J = 8 Hz, 2H), 7.28 (t, J = 8 Hz, 1H). ^{13}C NMR (100 MHz, DMSO-d_6) δ (ppm): 186.43, 162.31, 138.47, 128.58, 126.82, 123.41. All NMR spectra coincide with the literature data [86].

Benzothiazole-2-carboxamide. To the suspension of $K_3Fe(CN)_6$ (215.00 g, 653.00 mmol) in water (400 mL) the solution of 2-(phenylamino)-2-thiooxoacetamide (9.20 g, 51.1 mmol) in 10% aq NaOH (810 mL) was added under stirring. Suspension was stirred for 1 h at room temperature and filtered. Brown product was filtered, washed with water and dried on air. Yield 6.37 g (70%). Light brown powder. R_f (DCM:MeOH 3:1) 0.66.^{1}H NMR (400 MHz, DMSO-d_6) δ (ppm): 8.48 (s, 1H), 8.20 (d, J = 8 Hz, 1H), 8.11 (d, J = 8 Hz, 1H), 8.07 (s, 1H), 8.20 (d, J = 8 Hz, 1H), 7.61 (t, J = 8 Hz, 1H), 7.55 (t, J = 8 Hz, 1H). ^{13}C NMR (DMSO-d_6) δ (ppm): 165.01, 161.35, 152.85, 136.40, 127.04, 126.66, 124.02, 123.01. All NMR spectra coincide with the literature data [86].

Potassium benzothiazole-2-carboxylate was obtained according to Scheme 1. The benzothiazole-2-carboxamide (6.40 g, 35.8 mmol) were mixed with 10% aq KOH (194 mL) and refluxed for 45 min. Reaction mixture was filtered while hot and cooled to room temperature. Precipitate was filtered, washed with water and dried. Yield 4.15 g (53%). Beige flakes. Mp. > 360 °C (dec.). $C_8H_5NO_2S$: HRMS, *m/z*: calcd. for $[M - H]^-$, 162.0197; found, 162.0189. IR (KBr, cm^{-1}): 3233, 1613, 1491, 1362, 1316, 1125, 845, 757, 731.^{1}H NMR (400 MHz, D_2O) δ (ppm): 7.80 (d, J = 8 Hz, 1H), 7.73 (d, J = 8 Hz, 1H), 7.36 (t, J = 8 Hz, 1H), 7.29 (t, J = 8 Hz, 1H). ^{13}C NMR (100 MHz, D_2O) δ (ppm): 167.23, 165.93, 152.05, 136.02, 126.66, 126.58, 123.36, 122.32. Calcd: C, 53.62; H, 2.81; N, 7.82%; found: C, 53.57; H, 2.76; N, 7.92%.

2.3.3. Synthesis of lanthanide complexes (Ln = Eu^{3+}, Gd^{3+}, Tb^{3+})

Synthesis of Ln(boz)$_3$·3H$_2$O. To the solution potassium benzoxazole-2-carboxylate (0.06 g, 0.30 mmol) in acetone (10 mL) the solution

lanthanide chloride hydrate (0.05 g, 0.12 mmol) in acetone (10 mL) was added. After prolonged stirring, the precipitate was filtered off. The filtrate was evaporated to dryness, redissolved in water (30 mL) and evaporated to dryness. Yield 0.05 g (65%). Pale brown powder.

Eu(boz)$_3$·3H$_2$O: Calcd. for $EuC_{24}H_{16}N_3O_{11}$: C 41.63, H 2.62, N 6.07%; found: C 41.78, H 2.56, N 6.13%. IR (KBr, cm^{-1}): 3279, 1650, 1545, 1393, 1332, 1256, 1164, 845, 741.

Gd(boz)$_3$·3H$_2$O: Calcd. for Gd $C_{24}H_{16}N_3O_{11}$: C 41.32, H 2.60, N 6.02%; found, %: C 41.48, H 2.66, N 6.18. IR (KBr, cm^{-1}): 3280, 1649, 1539, 1385, 1334, 1252, 1158, 843, 737.

Tb(boz)$_3$·3H$_2$O: Calcd. for Tb $C_{24}H_{16}N_3O_{11}$: C 41.22, H 2.59, N 6.01%; found %: C 41.65, H 2.61, N 6.07. IR (KBr, cm^{-1}): 3279, 1649, 1543, 1387, 1329, 1253, 1162, 842, 735.

Synthesis of Ln(btz)$_3$·3H$_2$O. To the solution lanthanide chloride hexahydrate (0.05 g, 0.12 mmol) in water (5 mL) the solution of the potassium benzothiazole-2-carboxylate (0.1 g, 0.46 mmol) in water (10 mL) was added. The precipitate was filtered and dried on air. Yield 0.07 g (70%). White powder.

Eu(btz)$_3$·3H$_2$O: Calcd. for $EuC_{24}H_{18}N_3O_9S_3$: C 38.92, H 2.45, N 5.67%; found: C 39.04, H 2.38, N 5.51%.IR (KBr, cm^{-1}): 3232, 1611, 1490, 1364, 1315, 1131, 844, 758, 728.

Gd(btz)$_3$·3H$_2$O: Calcd. for $GdC_{24}H_{18}N_3O_9S_3$: C 38.65, H 2.43, N 5.63%; found: C 38.93, H 2.44, N 5.72%. IR (KBr, cm^{-1}): 3234, 1615, 1487, 1362, 1317, 1129, 847, 757, 732.

Tb(btz)$_3$·3H$_2$O: Calcd. for $TbC_{24}H_{18}N_3O_9S_3$: C 38.56, H 2.43, N 5.62%; found: C 38.62, H 2.45, N 5.59%. IR (KBr, cm^{-1}): 3237, 1617, 1497, 1359, 1312, 1125, 855, 764, 725.

Synthesis of Eu(boz)$_3$·Q, Q = Phen, BPhen (Phen – 1,10- phenanthroline, BPhen – 4,7-diphenyl-1,10-phenanthroline). To the solution lanthanide chloride hexahydrate (0.05 g, 0.12 mmol) in acetone (10 mL) the solution of Phen/BPhen (0.02/0.05, 0.12 mmol) in acetone (10 mL) was added. After prolonged stirring, the solution of 0.06 g of potassium benzoxazole-2-carboxylate in 10 mL of acetone was added to a mixture. Then mixture was stirred for 30 min and the precipitate was filtered off. The filtrate was evaporated to dryness, redissolved in 30 mL of water and evaporated on a rotary evaporator. Yield 0.05/0.05 g (48/41%). Pale brown powder.

Eu(boz)$_3$·Phen: Calcd. for $EuC_{24}H_{16}N_3O_{11}$: C 52.81, H 2.44, N 8.56, found: C 51.96, H 2.38, N 8.60%. IR (KBr, cm^{-1}): 3186, 1653, 1540, 1381, 1328, 1249, 1004, 840, 730.

Eu(boz)$_3$·BPhen: Calcd. for $EuC_{24}H_{16}N_3O_{11}$: C 59.38, H 2.89, N 7.22, found: C 58.98, H 2.93, N 7.27%. IR (KBr, cm^{-1}): 3203, 1642, 1542, 1382, 1330, 1248, 1160, 841, 741, 702.

Synthesis of Eu(btz)$_3$·Q, Q = Phen, BPhen. To the solution lanthanide chloride hexahydrate (0.045 g, 0.12 mmol) in water (10 mL) the solution of Phen/BPhen (0.022/0.045 g, 0.12 mmol) in ethanol (10 mL) was added. After prolonged stirring, solution of the potassium benzothiazole-2-carboxylate (0.1 g, 0.46 mmol) in water (10 mL) was added to the mixture. The precipitate was filtered and dried on air. Yield 0.08/0.09 g (75%). White powder.

Eu(btz)$_3$·Phen: Calcd. for $EuC_{24}H_{16}N_3O_8S_3$: C 49.88, H 2.31, N 8.08, found: C 50.01, H 2.35, N 8.02%. IR (KBr, cm^{-1}): 3255, 1624, 1493, 1364, 1314, 1127, 845, 760, 730.

Eu(btz)$_3$·BPhen: Calcd. for $EuC_{24}H_{16}N_3O_8S_3$: C 56.58H 2.77, N 6.87, found: C 56.61, H 2.76, N 6.91%. IR (KBr, cm^{-1}): 3135, 1620, 1494, 1358, 1315, 1113, 835, 762, 701.

Cellular uptake. Confocal microscopy (using a Leica SPE Scanning confocal inverted microscope) was performed in order to investigate the cellular uptake and the distribution of the compounds. Therefore, HeLa (human cervical carcinoma) cells were seeded in 8-well μ-chamber slides (ibidi) the at the density of 2×10^4 cells/well in DMEM (Gibco) supplemented with 10% FCS (Gibco) and 1% penicillin/streptomycin (Gibco). After 24 h of incubation at 37 °C, 5% CO_2, the medium was removed and the cells were treated with the compounds (10 μM) in DMEM and incubated for 72 h at 37 °C, 5% CO_2. For the negative control, the cell culture medium was exchanged in some wells without addition of the compounds. After incubation, cells were washed three times with DPBS (Gibco). The compounds were excited at 405 nm, emission was measured at 550–750 nm. Images were taken as sequential scans at 400 Hz with a resolution of 1024 × 1024 pixels.

Cytotoxicity studies. HeLa (human cervical carcinoma) cells were seeded in the 96 well plates at the density of 1×10^4 cells/well in DMEM (Gibco) supplemented with 10% FCS (Gibco) and 1% penicillin/streptomycin (Gibco). After 24 h of incubation at 37 °C, 5% CO_2, the medium was removed and the cells were treated with various concentrations of the complexes in DMEM (solvent concentration ≤ 0,5% v/v) and incubated for 72 h at 37 °C, 5% CO_2. For the negative control, the cell culture medium was exchanged in some wells without addition of the compounds, for the solvent control the corresponding amount of the solvent was added. Thereafter, 15 μl of the MTT reagent (Promega) were given in each well. For the positive control, Triton X-100 (1%) (Serva) was added in some wells before treating them with the MTT reagent. After 3 h of incubation the cells were lysed using the Stop Solution (Promega) to release the blue-purple formazan. The cell viability was determined by measuring the absorbance of the resulting formazan at 595 nm using a multiwell plate reader (SpectraMax ID3, Molecular Devices, USA) and calculated in relation to the negative/solvent control.

3. Results and discussion

Synthesis of heteroaromatic acids. Both acids were prepared in the form of potassium salts since the corresponding acids are unstable against decarboxylation in acidic environment [87]. Benzoxazole-2-carboxylate was synthesized by ring closure reaction of ortho-ester with 2-aminophenol [88] with subsequent hydrolysis of obtained methyl ester. Benzothiazole-2-carboxylate was synthesized by the novel approach consisting of the sequential alkylation-oxidation of aniline [89] and oxidative ring closure with potassium ferricyanide [90] followed by hydrolysis. This approach was proved effective and will allow obtaining other substituted benzothiazoles from commercially available anilines. The composition of the obtained compounds was established based on ^{1}H and ^{13}C NMR data; in addition, single crystals of 2-(phenylamino)-2-thiooxoacetamide and methyl benzoxazole-2-carboxylate were obtained (CCDC 1887593 and 1887587; see Electronic Supporting Information (ESI); Figure S1, Figure S2).

Lanthanide complexes Ln(btz)$_3$·3H$_2$O (Ln = Eu, Gd, Tb) were obtained by the interaction between aqueous solutions of potassium benzothiazole-2-carboxylate and lanthanide chloride hexahydrate solution. While Ln(boz)$_3$·3H$_2$O (Ln = Eu, Gd, Tb) were obtained by the same exchange reaction in acetone due to K(boz) was insoluble in water. The obtained complexes were recrystallized from water to avoid toxic acetone in their composition. It turned out that Ln(boz)$_3$·3H$_2$O rapidly degraded in water solution which was obvious from fast decrease of product yield. In contrast, Ln(btz)$_3$·3H$_2$O was stable in the solution.

Mixed-ligand (ML) lanthanide complexes Eu(carb)$_3$·Q (carb = boz, btz, Q = Phen, BPhen) were obtained by the reaction between $EuCl_3$Q (*in situ* from $EuCl_3.6H_2O$ and Q in EtOH) and corresponding K(carb) in ethanol. The ML complexes precipitated from ethanol, were filtered off, washed with ethanol and dried in air.

According to the XRD data all the complexes Ln(carb)$_3$·3H$_2$O and Eu(carb)$_3$·Q (Ln = Eu, Gd, Tb; carb = boz, btz, Q = Phen, BPhen) were amorphous (Figure S6; Figure S7), which is important for OLED, as crystallization of the emission layer would immediately result in the device shorting. Thus their composition was determined by combination of TGA and elemental analyses, ^{1}H NMR spectroscopy and IR spectroscopy. The TGA data of Ln(carb)$_3$·Solv (Ln = Eu, Gd, Tb; carb = boz, btz) was carried out in the temperature range 200–800 °C; mass-spectrometry of released gases was used (mass numbers 18 (H_2O), 44 (CO_2), 58 (MeC(O)Me)). It was shown that Ln(boz)$_3$·Solv (Ln = Eu, Gd, Tb) obtained from acetone contained both coordinated water and

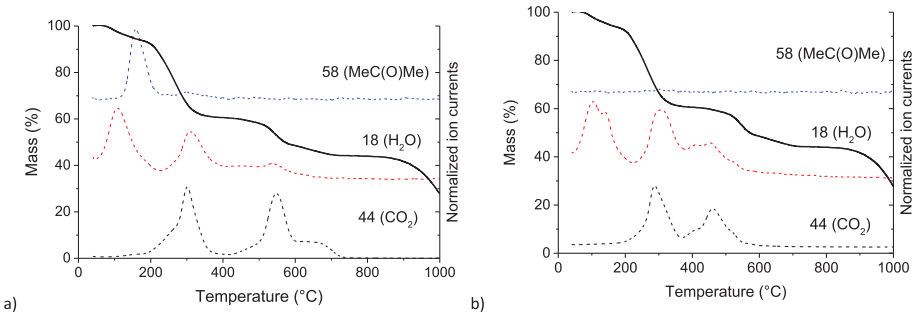

Fig. 2. TGA data with normalized ionic currents of a) $Eu(boz)_3$·Solv, b) $Eu(boz)_3·3H_2O$.

acetone molecules, while in the TGA pattern of $Ln(boz)_3·3H_2O$ (Ln = Eu, Gd, Tb), recrystallized from water, acetone ionic current (M = 58) demonstrated no maxima, witnessing the success of recrystallization in avoiding acetone presence (Fig. 2). Hydrate composition of $Ln(carb)_3·3H_2O$ (Ln = Eu, Gd, Tb; carb = boz, btz) was determined from the weight loss in the temperature range of ca. 50–200°, determined from water ionic current, and confirmed by elemental analysis. Water coordination was also evident from the IR spectroscopy data (Figure S3).

TGA data of ML complexes proved the absence of coordinated water molecules and the presence only one neutral ligand according to weight loss (clcd 22% vs found 25% for Phen loss, clcd 33% vs found 30% for BPhen loss) in the range of 200–400°C (Fig. 2; Figure S4; Figure S5).

^{1}H NMR spectroscopy of homoligand complexes in bioinert solvents (water and DMSO) was used to prove the presence of the metal-to-ligand bond in solution, which would ensure the sensitization of europium ionic luminescence and ensure bright luminescence of the complex in solution, which is important i.e. for bioimaging application. This is possible due to the shift and broadening of the proton signals occur in the ^{1}H NMR spectra, if the ligand, to which the protons belong, is coordinated by the europium ion, which is due to the europium magnetic moment, of the europium CC. While in the case of complete dissociation there is no influence of the ligand proton signals on the europium ion luminescence [91–93]. As a result of partial dissociation, there would be both coordinated and non-coordinated carboxylate anions present in the solution; however fast exchange [$Eu(carb)_3 \leftrightarrow Eu(carb)_{3-x}^{x+} + x\,(carb)^-$] results in the presence of only one set of signals, their position intermediate between that of free and coordinated $(carb)^-$. For example, fluorobenzoates demonstrated complete dissociation in water, metal to ligand bonds were observed only in organic solvents [24,94].

Indeed, ^{1}H NMR spectra of $Eu(carb)_3·3H_2O$ (carb = boz, btz) in D_2O revealed the proton signals shifts; their values depended on the proton position (Fig. 3b). So, the largest shift (ca. 0.4 ppm) was observed for proton (1) (Fig. 3a) for both $Eu(carb)_3·3H_2O$ (carb = boz, btz) witnessing not only the presence of the Eu–carb bond, but also the nitrogen atom participation in the coordination. Indeed, in the absence of the heteroatom coordination, such as for europium benzofuranoate, both protons of the benzene ring (1) and (4) underwent the same shift (Figure S9) [72]. The reason for the presence of N,O-coordination of lanthanide atom and the absence of E,O-coordination (E = O, S) of lanthanide atom is apparently the possibility of decoupling an unbound electron pair by the nitrogen atom, while oxygen or sulfur have a saturated electron shell, which is not capable of forming a bond with lanthanide atom. Indeed, according to CSD, O and S heteroatom coordination is untypical, unlike N heteroatom coordination.

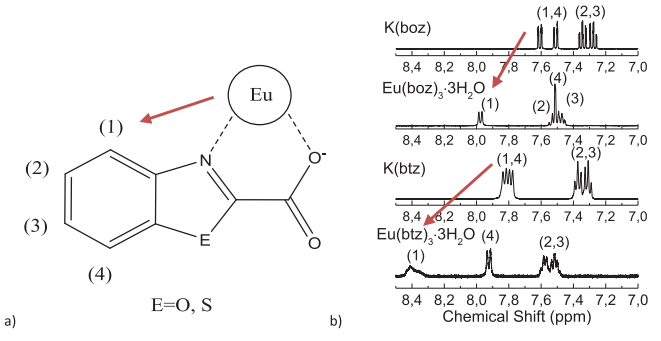

Fig. 3. a) Proton numbering and suggested ligand coordination mode and b) ^{1}H NMR spectra of K(carb) (5 g/L) and $Eu(carb)_3·3H_2O$ (2 g/L) in D_2O (carb = boz, btz).

^{1}H NMR spectra of ML complexes also approved the suggested composition $Eu(carb)_3$·Q (carb = boz, btz; Q = Phen, BPhen) according to the integral intensity ratio of anionic and neutral ligand proton signals (Figure S10; Figure S11).

Solubility of the obtained complexes was measured in H_2O, C_2H_5OH, MeC(O)Me, MeOH, $CHCl_3$ which is important for OLED thin film deposition (C_2H_5OH, MeC(O)Me, MeOH, $CHCl_3$) and for bioimaging (H_2O) (Table 1). It turned out that the heteroatom introduction into the aromatic ligand keeps high solubility of complexes even when ligand conjugated length increases for both ligands. Thus, the solubility of $Eu(carb)_3·3H_2O$ (carb = boz^-, btz^-) reaches 2.2–2.4 mmol/L which is lower than of fluorobenzoates [23,24,94], but higher than of the whole number of europium aromatic carboxylates, i.e. 3,4-dimethoxybenzoate $Eu(dmb)_3·4H_2O$ (0.97 mmol/L) [66] and naphthoate $Eu(nph)_3·2H_2O$ (0.0353 mmol/L) [95]. Solubility in organic solvents is even higher and riches 20.2 mmol/L for $Eu(btz)_3·3H_2O$ in chloroform. This is an indirect proof of the presence of the N–Eu bond.

Neutral phenanthroline-based ligand introduction decreases the solubility: so, water solubility of ML complexes is too low to be measured. Nevertheless, the solubility in ethanol and chloroform still reaches 5 mmol/L, which is enough for thin film deposition.

So, ligand design allows us to obtain highly soluble complexes in organic solvents and water, which did not completely dissociate in solution due to suggested N,O-coordination.

The ligand optical absorption determination revealed that molar extinction coefficient was, indeed, very high and reached $\varepsilon(\lambda = 275\,nm) = 13500\ (M\,cm)^{-1}$ for K(boz), while for K(btz) was slightly lower (Fig. 4a). For comparison, ε (λ = 265 nm) = 500 $(M\,cm)^{-1}$ and (λ = 270 nm) 4000 $(M\,cm)^{-1}$ were measured for pentafluorobenzoate [24] and benzoate anions [51], correspondingly. Both homoligand europium complexes demonstrated ε up to 60000 $(M\,cm)^{-1}$, which ensures their visually bright luminescence. Even the introduction of highly absorbing Phen ligand did not further increase absorption, unlike Phen-containing fluorobenzoates [16,23]. The use of BPhen instead of Phen resulted in $Eu(btz)_3$·BPhen absorption up to 10^5 $(M\,cm)^{-1}$, which is a very high value.

Luminescent properties. Prior to examination of the luminescence properties of Tb^{3+} and Eu^{3+} complexes, triplet states of the obtained ligands were determined from the phosphorescence spectra of corresponding $Gd(carb)_3·3H_2O$ ($carb^-$ = boz^-, btz^-) from the maximum of the 0-0 phonon band [34,38,58,96] (Figure S12). The triplet states of both ligands were about 20400 cm^{-1}, demonstrating no dependence on

Table 1
Solubility of europium complexes (mmol·L^{-1}/g·L^{-1}).

Sample	Eu(bfc)$_3$·3H$_2$O[a]	Eu(boz)$_3$·3H$_2$O	Eu(boz)$_3$·Phen	Eu(boz)$_3$·BPhen	Eu(btz)$_3$·3H$_2$O	Eu(btz)$_3$·Phen	Eu(btz)$_3$·BPhen	Eu(dmb)$_3$·4H$_2$O [108]	Eu(pfb)$_3$·H$_2$O [24]	Eu(nph)$_3$·2H$_2$O [95]
H$_2$O	1.4/1.0	2.2/1.5	0.5/0.4	0.1/0.1	2.4/1.8	0.2/0.2	0.1/0.1	0.97/0.75	68.5/55.21	0.035/0.02
C$_2$H$_5$OH	6.2/4.3	11.5/8.0	6.1/5.0	5.2/5.0	9.5/7.0	5.8/5.0	4.9/5.0	n/a	n/a	n/a
Me$_2$C(O)	0.58/0.4	2.6/1.8	n/a	n/a	1.4/1.0	n/a	n/a	n/a	n/a	n/a
MeOH	4.6/3.2	15.9/11.0	n/a	n/a	3.5/2.6	n/a	n/a	n/a	n/a	n/a
CHCl$_3$	5.5/3.8	17.3/12.0	4.9/4.0	4.1/4.0	20.2/15	4.6/4.0	4.9/5.0	n/a	n/a	n/a

n/a – not available.
[a] Eu(bfc)$_3$·3H$_2$O was obtain in previous work [72] and tested in the present work for comparison.

second heteroatom, and should be optimal for sensitization of Eu^{3+} luminescence [97] and coincided with the excited state energy of Tb^{3+}.

In the case of Tb(carb)$_3$·3H$_2$O for both carb = boz, btz pure terbium ionic luminescence was observed, carb$^-$ luminescence was not present in the spectra (Fig. 5b). However, the quantum yield of terbium luminescence reached only 1–2% (Table S 1). At the same time, Tb(boz)$_3$·Solv obtained from acetone (Table S 1), demonstrated quantum yield of 20%, which seem to witness the quenching role of water molecules. However, water quenches terbium luminescence rather ineffectively; so, benzoate hydrate [98], phenoxybenzoate hydrate [40], pyrazolecarboxylate hydrate [20] of terbium demonstrate quantum yields up to 100%. We suggest that in present case we observe the cumulative quenching effect by the ligand, which provides the back energy transfer, and the water molecules. The same effect was observed in the case of Tb(carb)$_3$·Phen [99], containing hydroxocarboxylate anions (carb): they demonstrated low intensity or no terbium luminescence at room temperature due to the cumulative effect of OH-groups in the composition of anionic ligand and Phen molecules. This suggestion

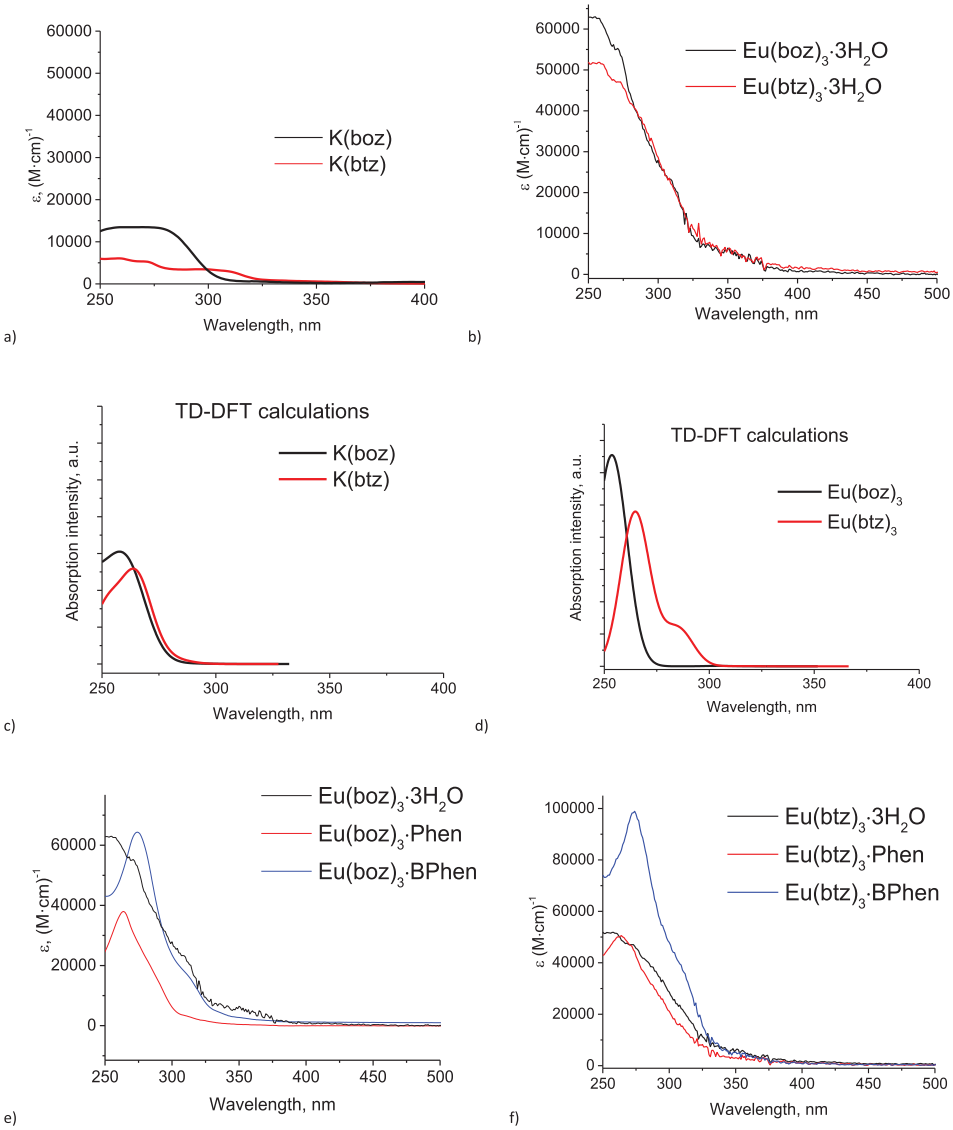

Fig. 4. Absorption spectra of a) K(carb) (acetonitrile, 10^{-5} M), b) Eu(carb)$_3$·3H$_2$O (EtOH, 10^{-5} M), c) K(carb) (TD-DFT calculated) d) Eu(boz)$_3$ (TD-DFT calculated) e) Eu(boz)$_3$·Q (EtOH, 10^{-5} M), (Q = Phen, BPhen) f) Eu(btz)$_3$·Q (EtOH, 10^{-5} M), (Q = Phen, BPhen).

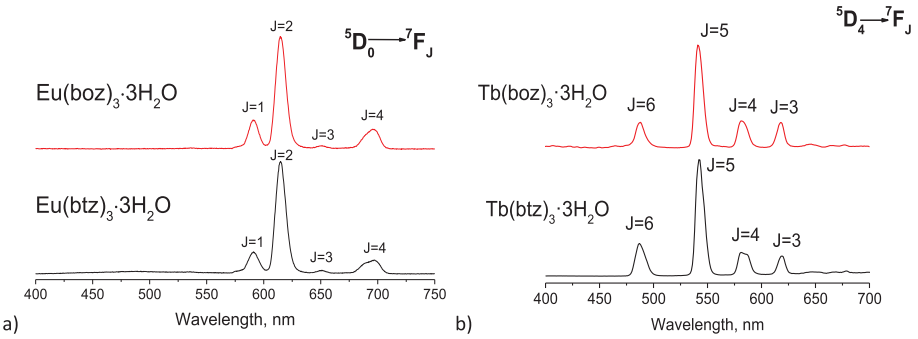

Fig. 5. Luminescence spectra (λ_{ex} = 337 nm) at 298 K a) of Eu(carb)$_3$·3H$_2$O (carb = boz, btz), b) of Tb(carb)$_3$·3H$_2$O (carb = boz, btz).

is supported by the absence of ligand luminescence in the spectra (Fig. 5b) as well as by much higher quantum yields of europium complex luminescence, since europium is known to be quenched by water molecules much more effectively [100–102]. In case of benzofuranoates [103] terbium complex demonstrated low luminescence intensity at room temperature due to back energy transfer (Tb → carb) was dominating, which was indicated by presence of ligand luminescence in the spectra.

The cumulative influence of the back energy transfer and vibrational quenching is solidly demonstrated by the study of luminescence thermal dependence in solution. While the intensity of europium luminescence is almost independent on temperature in ethanol and almost independent even in water, terbium luminescence decreases significantly in water, ethanol, chloroform and acetone upon heating, witnessing that back energy transfer is responsible for this behavior. The value of the luminescence intensity decrease depends on the solvent, witnessing the role of OH-vibrational quenching.

Such a behavior allowed suggesting these complexes for luminescent thermometry applications.

The solutions in ethanol, containing the mixture of xEu(btz)$_3$·3H$_2$O and (1-x)Tb(btz)$_3$·3H$_2$O with x = 0.01 and 0.025 were tested as luminescence thermometry materials (Fig. 6). As the luminescence intensity ratio (LIR) the ratio between the intensities of terbium and europium luminescence bands at 545 and 612 nm, correspondingly, was taken. While the sensitivity of the obtained systems was characterized by the commonly used parameter S_r = 1/LIR(dLIR/dT), where T is temperature [104,105]. Both systems demonstrated S_r values up to 2.4–2.8, which are rather high: indeed, the sensitivity of 2.8 in the physiological range (35–50°C) is the highest obtained for the Tb–Eu system. This is not surprising: as some of us have theoretically shown [106] and experimentally verified [107], the sensitivity of the thermometer based on the energy transfer between Tb and Eu only depends on temperature and is limited by ca. 0.5%/K in the physiological range. In the present system the ligand triplet state is involved in the temperature-dependent luminescence processes, which allows the significant increase in the sensitivity up to the record value. Important is that the luminescence is reversible when the samples were cooled down to its original temperature (Figure S28).

It is also important that the sensitivities of both systems are very similar despite very different LIR values. This allows suggesting that in 4-level systems (ground state + 3 excited states, i.e. of Tb, Eu and btz ligand) the sensitivity is also dependent only on the level energies and temperature.

Both europium carboxylate hydrates demonstrated solely europium luminescence with the quantum yields of 7%, which is higher than of terbium complexes, additionally speaking in favour of the suggested mechanism of terbium luminescence quenching. These quantum yields, though rather moderate, were not limited by quenching of the water molecules. Indeed, introduction of the neutral ligands – both *o*-phenanthroline (Phen) and batophenanthroline (BPhen) – into the europium coordination sphere resulted in a very moderate increase of the quantum yield (in case carb = btz) or even decrease of the quantum yield (carb = boz). At the same time sensitization efficiency reaches 50%, which means that quantum yields of all complexes Eu(carb)$_3$Q (carb = boz, btz; Q = 3H$_2$O, Phen, BPhen) was caused by a quenching mechanism, which is, however, not associated with water OH vibrations.

The latter conclusion was supported by the values of luminescence lifetimes which were almost independent on the neutral ligand Q in the europium coordination sphere (Q = H$_2$O, Phen, BPhen) and rather slightly depended on the anionic ligand (boz, btz) (Table S 1).

Despite rather low quantum yield values, luminescence intensity of europium and terbium complexes was visually bright due to the high absorption of the ligands. Indeed, luminosity $L = \varepsilon * PLQY$ of the complexes reached 9800 $(M\,cm)^{-1}$; this is lower than luminosity of europium 2-fluorobenzoate with phenanthroline (26550 $(M\,cm)^{-1}$) with the record quantum yield among europium complexes, however, is higher than that of some widely known luminescent materials as europium complexes with dipicolinate [43] and salicylic derivates [109].

Thus, ligand design allowed obtaining brightly luminescent europium complexes due to the ligand high absorption, though the PLQY values turned out to be rather moderate. This allowed successfully using them as bioimaging materials (see Figure S 18).

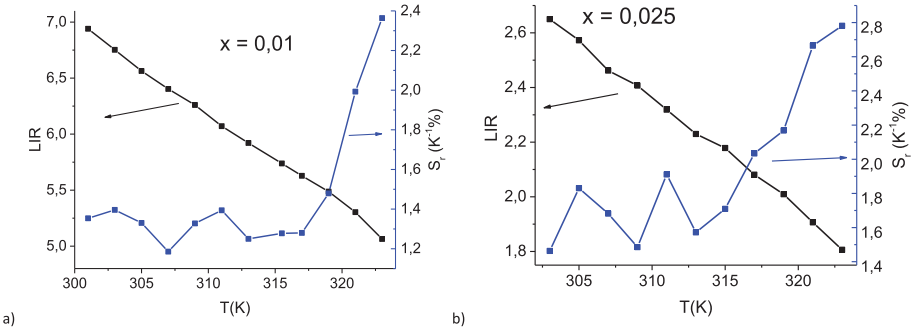

Fig. 6. LIR and S values of Eu$_x$Tb$_{1-x}$(btz)$_3$·3H$_2$O, dissolved in ethanol (2.5 g/l):a) x = 0.01 and b) x = 0.025.

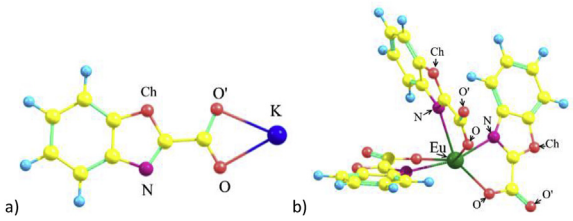

Fig. 7. DFT optimized geometry of K(carb) (a) and Eu(carb)$_3$ (b) molecules (carb = boz. btz).

Quantum chemical calculations. Since the X-ray structures of considered metal carboxylates were not available, we have performed a series of DFT calculations to determine the geometry. First of all, the most energetically favourable carb$^-$ coordination mode, namely O,O'; O, Ch or O,N, was determined (see Fig. 7a for atom assignment).

The localization and the energy of frontier orbitals, HOMO and LUMO, are of crucial importance for luminescent molecules use in OLEDs. It is well known that the DFT method, suitable for ground state calculations, significantly overestimates the energies of virtual orbitals containing no electrons, to which the LUMO belongs. Therefore, in our work we used a dual-stage approach to determine the LUMO energy, based on the calculation of vertical excitations and then the energy gap (E_g) from TD-DFT, followed by the calculation of the LUMO energy as E (LUMO) = E(HOMO) + E_g as reported in previous work of some of us [39]. To verify the reasonableness of vertical excitation calculations, the TD-DFT absorption spectra were compared with those experimentally observed and were found to be in a good agreement as described above (Fig. 4).

Therefore, accurate calculations of HOMO and especially LUMO energy levels for voluminous Eu tris-carboxylates in the framework of DFT and TD-DFT require remarkable computation resources. One can expect that ionic bond nature in both rare earth and alkaline carboxylates, as well as the localization of frontier orbitals on organic ligand species, make it possible to perform calculation of K(carb) molecules instead of Eu(carb)$_3$ to simplify the system. In the present work, we have performed calculation of HOMO and LUMO levels for both K and Eu carboxylates to check the correctness of this simplification to reveal the impact of central ion on coordination mode and frontier molecular orbitals.

DFT calculations of K(carb) molecules (carb = boz, btz) revealed that the geometry with bidentate O,O' coordination mode of carb$^-$ has the lowest energy (Fig. 7), while the structure containing O,N or O, Ch coordinated ligand is less favourable (Table S 1). In contrast to K(carb), for Eu(carb)$_3$ the N,O ligand coordination is energetically favourable (Fig. 7b, Table S 1). This difference the most probably originates from the smaller ionic radius of Eu^{3+} (1.17 Å for CN = 6) rather than of K^+ (1.38 Å) which is comparable with the bite size of carb ligand (2.70 Å). Therefore, based on the combination of theoretical DFT results and experimental data of ^{1}H NMR and solubility measurements we can conclude the participation of nitrogen heteroatom in the coordination of europium ion.

Difference in coordination mode of carb$^-$ and especially in number of coordinated ligands in molecules of K(carb) and Eu(carb)$_3$ resulted in different localization of frontier orbitals. So, in K(carb) HOMO is localized on the organic ligand (Fig. 8a), while LUMO is mostly localized

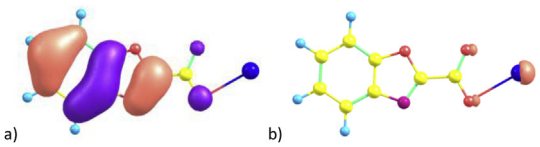

Fig. 8. Localization of HOMO (a) and LUMO (b) of K(boz) based on DFT converged density.

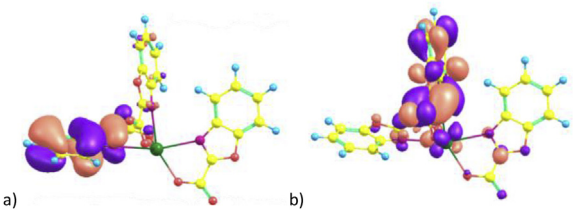

Fig. 9. Localization of HOMO (a) and LUMO (b) of Eu(boz)$_3$ based on DFT converged density.

Table 2
DFT and TD-DFT calculated energy levels of frontier molecular orbitals for K (carb) and Eu(carb)$_3$, (carb = boz. btz).

	HOMO. eV	Gap. eV	LUMO[a]. eV
K(boz)	−6.128	4.443	−1.685
K(btz)	−6.027	4.331	−1.696
Eu(boz)$_3$	−7.554	4.751	−2.803
Eu(btz)$_3$	−7.322	4.294	−3.028

[a] - estimation of LUMO energy value is done on the basis of HOMO level and Gap values.

on the potassium ion (Fig. 8b).

For both europium complexes, HOMO and LUMO are localized on different organic ligands in europium coordination sphere (Fig. 9). This significantly reduces the energy levels of HOMO and LUMO by ca. 1.5eV (Table 2) and makes it impossible to use the energies calculated for K(carb) as an estimation of those for Eu(carb)$_3$ (See ESI for more details).

According to DFT and TD-DFT results, Eu(boz)$_3$ and Eu(btz)$_3$ molecules demonstrate quite similar values of frontier orbital energies. However, it is worth noting that HOMO level of Eu(btz)$_3$ is by ca. 0.2 eV higher, that is not important for photoluminescence properties but may play an important role in OLED.

Thus, the obtained europium CCs possessed photoluminescence and sufficient solubility, and they can be expected to demonstrate the charge carrier mobility as a consequence of the electron-depleted heteroaromatic ring system and the dipole-dipole interaction of conjugated systems presence, and their HOMO and LUMO energies were calculated. This made it possible to test the europium CC as a material for the emission layer in OLED devices.

OLED preparation and testing. Calculated HOMO energies are very low, which made it impossible to properly select the hole-transport layer (HTL) for OLED fabrication based on these values. Thus, poly-TPD was selected as hole transport layer due to its insolubility in most solvents after post-treatment (annealing at 220 °C for 30 min in argon-glovebox atmosphere) [110], which allowed us to investigate solvent influence on emission layer (EML) performance in OLED. As electron transport layer (ETL) well known and often used TPBi material was selected [5,23,39,111].

So, OLED devices with heterostructure ITO/PEDOT-PSS/poly-TPD/EML/TPBi/LiF/Al, where EML = Eu(carb)$_3$Q (carb = boz, btz, Q = 3H$_2$O, as well as Phen and BPhen), were obtained (Table 3). The lifetimes of the emission layers coincided with those of powders,

Table 3
The list of obtained OLED devices.

Device designation	EML	Solvent
OLED 1	Eu(btz)$_3$·3H$_2$O	EtOH
OLED 2	Eu(btz)$_3$·3H$_2$O	CHCl$_3$
OLED 3	Eu(boz)$_3$3H$_2$O	EtOH
OLED 4	Eu(btz)$_3$·Phen	EtOH
OLED 5	Eu(btz)$_3$·BPhen	EtOH
OLED 6	Eu(btz)$_3$·BPhen	CHCl$_3$

obtained from corresponding solvents (see ESI). To be able to properly compare the performance of the obtained OLED devices, the electroluminescence (EL) spectra were measured at the same conditions (see Experimental section), only varying the integration time; thus, intensity is given in sec^{-1}, which corresponds to the counts divided by the integration time.

I–V curves of the devices with both EML = $Eu(carb)_3{\cdot}3H_2O$ (carb = boz, btz) demonstrated rather high current densities, witnessing that indeed the obtained complexes possessed enough charge carrier mobility proving our complex design hypothesis (Figure S19). At the same time only the device with EML = $Eu(btz)_3{\cdot}3H_2O$ possessed europium ionic luminescence, in contrast to the one with EML = $Eu(boz)_3{\cdot}3H_2O$. Indeed, as mentioned above, $Eu(boz)_3{\cdot}3H_2O$ is unstable in solution, so it may undergo rapid degradation in the thin film. In addition, it was shown, that $Eu(btz)_3{\cdot}3H_2O$ thin film obtained from ethanol demonstrated better EL performance than the one obtained from chloroform (Figure S20).

The presence of the poly-TPD emission band in the EL spectra of OLED1 and OLED2 reveals that electron-hole recombination occurs on the interface between EML and the hole transport layer. Indeed, it witnesses the electron, rather than hole, transport properties of EML; besides, due to very low HOMO level of EML, this layer plays rather hole-blocking role. Therefore, to improve the situation Phen and BPhen neutral ligands with relatively high HOMO energies were introduced to decrease HOMO-HOMO gap between poly-TPD and EML. It is worth noting that BPhen, known as ETL material, possesses own charge carrier mobility (Fig. 10).

Indeed, OLED devices with EML = $Eu(btz)_3{\cdot}Q$ (Q = Phen, BPhen) demontrated no poly-TPD luminescence (Fig. 11 (1), (2)). However, it turned out that Phen performed as an electron blocking layer due to the high LUMO energy. It was witnessed by the presence of TPBi emission band in the electroluminescence spectra, and resulted in the absence of the overall EL intensity increase. While BPhen introduction resulted in the disappearance of the parasitic HTL emission, and OLED5 and OLED6 demonstrated pure europium ionic electroluminescence, twice more intense than the one of OLED1 at the same current density; the solvent comparison again proved that ethanol is preferential over chloroform. Important is that PLQYs of $Eu(btz)_3{\cdot}Q$ (Q = $3H_2O$, Phen, BPhen) are similar (Table S 1), thus their different performance in OLEDs is due to different HOMO and LUMO energies.

So, the ligand design allowed us to obtain soluble europium CC with high enough electron mobility. Though their application in OLEDs was hampered by too low HOMO energy, introduction of neutral ligand allowed solving this problem. It is well-known that BPhen is usually used in order to increase efficiency of OLED device [7,25,112,113] because of its high electron mobility. However, in present work the I–V curves only differ in the V_{on} value due to the different HOMO-LUMO gaps of $Eu(btz)_3{\cdot}3H_2O$, Phen, and BPhen (Fig. 11) that indicates enough mobility of the designed carboxylate ligands, and BPhen helps solving the problem of too low HOMO energy.

4. Conclusions

The approach toward the directed synthesis of new lanthanide CC as a precursor to OLED emission layer material was proposed, and its effectiveness was shown. As such an approach, the combination of ligand conjugation extension together with heteroatom introduction was proposed. The appropriate selection of the heteroatom nature and position, namely the introduction of nitrogen heteroatom, able to be coordinated to lanthanide ions, in the α-position to the carboxy-group, allowed obtaining europium benzoxazole-2-carboxylates and benzothiazole-2-carboxylates with enough solubility and stability in solution, while the extended conjugation length together with the presence of two heteroatoms ensured both bright europium ionic luminescence and electron mobility. The properties of the obtained compounds were mainly independent on the second non-nitrogen heteroatom nature; the biggest difference was observed in the complex stability in solution, which made btz^- derivative prospective candidates to luminescent materials, unlike boz^- derivatives. At the same time, quantum yield was rather moderate, while HOMO energy was too high for effective electroluminescence; these obstacles were overcome by the neutral ligand introduction in the complex composition. As a result, mixed ligand $Eu(btz)_3{\cdot}$BPhen with effective electroluminescence was obtained.

Conflicts of interest

There are no conflicts to declare.

Acknowledgements

This work was supported by Russian Foundation for Basic Research (project №№ 18-33-00250, 16-53-76018).

The research is carried out using the equipment of the shared research facilities of HPC computing resources at Lomonosov Moscow State University. The luminescence thermometry investigations were financed by Russian Science Foundation (grant №17-73-10072).

AM and US thank the Research Training Group GRK2039.

Appendix A. Supplementary data

Supplementary data to this article can be found online at https://doi.org/10.1016/j.dyepig.2019.107604.

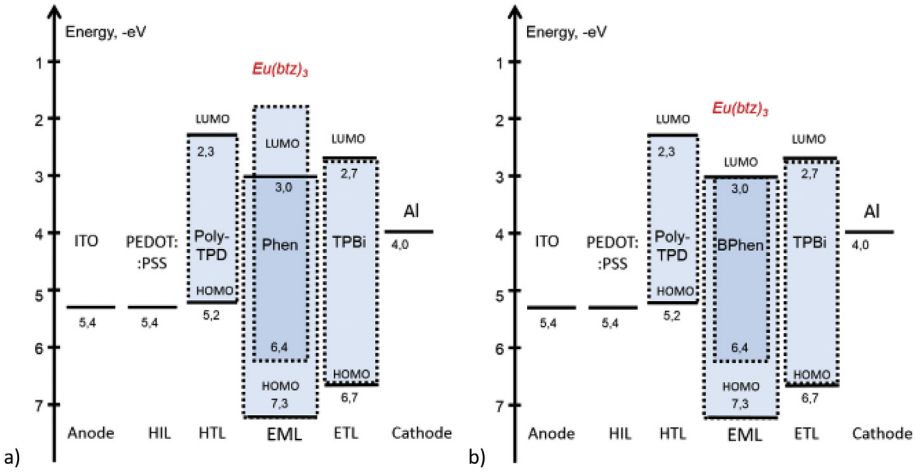

Fig. 10. The scheme of energy levels of obtained OLED devices with EML = $Eu(btz)_3{\cdot}Q$. Q = Phen. BPhen.

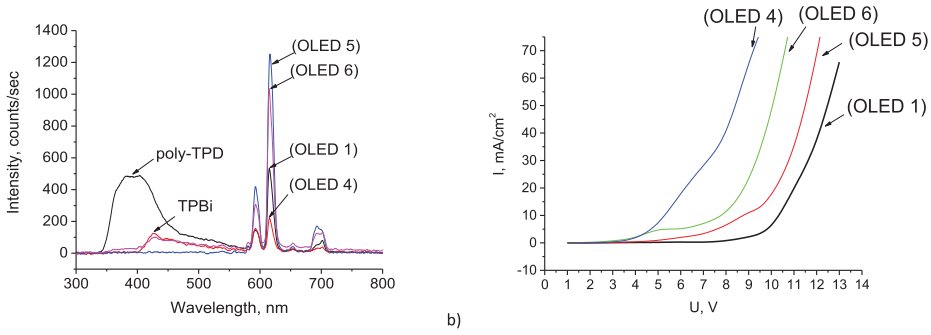

Fig. 11. a) The OLEDs electroluminescence spectra at 0.2 mA/mm^2: OLED 5, OLED 6, OLED 1, OLED 4 and b) their I–V curves.

References

[1] Crosby G a, Whan RE, Alire RM. Intramolecular energy transfer in rare earth chelates. Role of the triplet state. J Chem Phys 1961;34:743. https://doi.org/10.1063/1.1731670.

[2] Walzer K, Maennig B, Pfeiffer M, Leo K. Highly efficient organic devices based on electrically doped transport layers. Chem Rev 2007;107:1233–71. https://doi.org/10.1021/cr050156n.

[3] Zhang S, Turnbull GA, Samuel IDW. Highly efficient solution-processable europium-complex based organic light-emitting diodes. Org Electron 2012;13:3091–6. https://doi.org/10.1016/j.orgel.2012.09.006.

[4] Sun PP, Duan JP, Shih HT, Cheng CH. Europium complex as a highly efficient red emitter in electroluminescent devices. Appl Phys Lett 2002;81:792–4. https://doi.org/10.1063/1.1497714.

[5] Zhang L, Li B, Yue S, Li M, Hong Z, Li W. A terbium (III) complex with triphenylamine-functionalized ligand for organic electroluminescent device. J Lumin 2008;128:620–4. https://doi.org/10.1016/j.jlumin.2007.10.008.

[6] Yip Y, Wen H, Wong W, Tanner PA, Wong K. Increased antenna E ff ect of the lanthanide complexes by control of a number of terdentate N-donor pyridine ligands. Inorg Chem 2012;51:7013–5.

[7] Martín-Ramos P, Coya C, Álvarez ÁL, Ramos Silva M, Zaldo C, Paixão JA, Chamorro-Posada P, Martín-Gil J. Charge transport and sensitized 1.5 μm electroluminescence properties of full solution-processed NIR-OLED based on novel Er (III) fluorinated β-diketonate ternary complex. J Phys Chem C 2013;117:10020–30. https://doi.org/10.1021/jp402174s.

[8] Kuz'mina NP, Eliseeva SV. Photo and electroluminescence of lanthanide(III) complexes. Russ J Inorg Chem 2006;51:73–88. https://doi.org/10.1134/S0036023606010141.

[9] Jou JH, Ben Wang W, Chen SZ, Shyue JJ, Hsu MF, Lin CW, Shen SM, Wang CJ, Liu CP, Chen CT, Wu MF, Liu SW. High-efficiency blue organic light-emitting diodes using a 3,5-di(9H-carbazol-9-yl)tetraphenylsilane host via a solution-process. J Mater Chem 2010;20:8411–6. https://doi.org/10.1039/c0jm01163k.

[10] Esfahani H, Ghorbanpor M, Tanasan A. Implantable port devices, complications and outcome in pediatric cancer, a retrospective study. Iran. J. Pediatr. Hematol. Oncol. 2016;6:1–8. https://doi.org/10.1038/nature01430.1.

[11] Utochnikova VV, Grishko A, Vashchenko A, Goloveshkin A, Averin A, Kuzmina N. Lanthanide tetrafluoroterephthalates for luminescent ink-jet printing. Eur J Inorg Chem 2017;2017:1–6. https://doi.org/10.1002/ejic.201700896.

[12] Lammie PJ, Hightower AW, Richards FO, Bryan RT, Spencer HC, McNeeley DF, McNeeley MB, Eberhard ML. Alterations in filarial antigen-specific immunologic reactivity following treatment with ivermectin and diethylcarbamazine. Am J Trop Med Hyg 1992;46:292–5. https://doi.org/10.1063/1.120807.

[13] Krebs FC. Polymer solar cell modules prepared using roll-to-roll methods: knife-over-edge coating, slot-die coating and screen printing. Sol Energy Mater Sol Cells 2009;93:465–75. https://doi.org/10.1016/j.solmat.2008.12.012.

[14] Krebs FC, Gevorgyan SA, Alstrup J. A roll-to-roll process to flexible polymer solar cells: model studies, manufacture and operational stability studies. J Mater Chem 2009;19:5442–51. https://doi.org/10.1039/b823001c.

[15] Ahn SH, Guo LJ. High-speed roll-to-roll nanoimprint lithography on flexible plastic substrates. Adv Mater 2008;20:2044–9. https://doi.org/10.1002/adma.200702650.

[16] Kalyakina AS, Utochnikova VV, Zimmer M, Dietrich F, Kaczmarek AM, Van Deun R, Vashchenko AA, Goloveshkin AS, Nieger M, Gerhards M, Schepers U, Bräse S. Remarkable high efficiency of red emitters using Eu(+3) ternary complexes. Chem Commun 2018;54:5221–4. https://doi.org/10.1039/C8CC02930J.

[17] Junji K, Hiromichi H, Hongawa K, Nagai K, Katsuro O. Bright red light-emitting organic electroluminescent devices having a europium complex as an emitter. Appl Phys Lett 1994;2124:65. https://doi.org/10.1063/1.112810.

[18] Korshunov VM, Ambrozevich SA, V Taydakov I, Vashchenko AA. Dyes and Pigments Novel β -diketonate complexes of Eu 3 + bearing pyrazole moiety for bright photo- and electroluminescence. Dyes Pigments 2019;163:291–9. https://doi.org/10.1016/j.dyepig.2018.12.006.

[19] Utochnikova VV, Kuzmina NP. Photoluminescence of lanthanide aromatic carboxylates. Russ. J. Coord. Chem. Khimiya. 2016;42. https://doi.org/10.1134/S1070328416090074.

[20] Utochnikova VV, Kalyakina AS, Bushmarinov IS, Vashchenko AA, Marciniak L, Kaczmarek AM, Van Deun R, Bräse S, Kuzmina NP. Lanthanide 9-anthracenate: solution processable emitters for efficient purely NIR emitting host-free OLED. J Mater Chem C 2016;4:9848–55.

[21] Grishko AY, Utochnikova VV, Averin AA, Mironov AV, Kuzmina NP. Unusual luminescence properties of heterometallic REE terephthalates. Eur J Inorg Chem 2015;2015:1660–4. https://doi.org/10.1002/ejic.201403071.

[22] Utochnikova VV, Grishko AY, Koshelev DS, Averin AA, Lepnev LS, Kuzmina NP. Lanthanide heterometallic terephthalates: concentration quenching and the principles of the "multiphotonic emission. Opt Mater (Amst) 2017;74:1–8. https://doi.org/10.1016/j.optmat.2017.02.052.

[23] Utochnikova VV, Solodukhin NN, Aslandukov AN, Marciniak L, Bushmarinov IS, Vashchenko AA, Kuzmina NP. Lanthanide tetrafluorobenzoates as emitters for OLEDs: new approach for host selection. Org Electron 2017;44:85–93. https://doi.org/10.1016/j.orgel.2017.01.026.

[24] Kalyakina AS, Utochnikova VV, Bushmarinov IS, Ananyev IV, Eremenko IL, Volz D, Rönicke F, Schepers U, Van Deun R, Trigub AL, Zubavichus YV, Kuzmina NP, Bräse S. Highly luminescent, water-soluble lanthanide fluorobenzoates: syntheses, structures and photophysics, Part I: lanthanide pentafluorobenzoates. Chem - A Eur J 2016;21:17921–32. https://doi.org/10.1002/chem.201501816.

[25] Kalyakina AS, Sokolova EY, Vaschenko AA, Lepnev LS, V Utochnikova V, Kuzmina NP. High efficiency organic light-emitting diode based on UV stable terbium aromatic carboxylates. Proc. to SID Mid-Europe Chapter Spring Meet. 2013;1:19–20.

[26] Kalyakina AS, Utochnikova VV, Bushmarinov IS, Le-Deygen IM, Volz D, Weis P, Schepers U, Kuzmina NP, Bräse S. Lanthanide fluorobenzoates as bio-probes: a quest for the optimal ligand fluorination degree. Chem - A Eur J 2017;23:14944–53. https://doi.org/10.1002/chem.201703543.

[27] Utochnikova VV, Kalyakina AS, Lepnev LS, Kuzmina NP. Luminescence enhancement of nanosized ytterbium and europium fluorides by surface complex formation with aromatic carboxylates. J Lumin 2015;170:633–40. https://doi.org/10.1016/j.jlumin.2015.03.033.

[28] Utochnikova VV, Kalyakina AS, Solodukhin NN, Aslandukov AN. On the structural features of substituted lanthanide benzoates. Eur J Inorg Chem 2019;2019:2320–32. https://doi.org/10.1002/ejic.201801561.

[29] Cui Y, Chen B, Qian G. Lanthanide metal-organic frameworks for luminescent sensing and light-emitting applications. Coord Chem Rev 2014;273–274:76–86. https://doi.org/10.1016/j.ccr.2013.10.023.

[30] Shen L, Yang L, Fan Y, Wang L, Xu J. Constructions of a series of lanthanide metal-organic frameworks: synthesis, structure, luminescence and white light emission. CrystEngComm 2015. https://doi.org/10.1039/b000000x.

[31] Kotova O, Utochnikova V, Samoilenkov S, Kuzmina N. Thin films of Tb(pobz)3 (hpobz = 2-phenoxybenzoic acid): reactive CVD and optical properties. ECS Trans 2009;25:1107–14. https://doi.org/10.1017/CBO9781107415324.004.

[32] Kotova OV, Utochnikova VV, Samoylenkov SV, Rusin AD, Lepnev LS, Kuzmina NP. Reactive chemical vapour deposition (RCVD) of non-volatile terbium aromatic carboxylate thin films. J Mater Chem 2012;22:4897–903. https://doi.org/10.1039/C2JM13643K.

[33] V Utochnikova V, V Kotova O, Shchukina EM, V Eliseeva S, Kuz'mina NP. Gas-phase synthesis of terbium and lutetium carboxylates. Russ J Inorg Chem 2008;53:1878–84. https://doi.org/10.1134/S0036023608120085.

[34] Eliseeva SV, Bünzli J-CG. Lanthanide luminescence for functional materials and bio-sciences. Chem Soc Rev 2010;39:189–227. https://doi.org/10.1039/B905604C.

[35] Urgel JI, Cirera B, Wang Y, Auwärter W, Otero R, Gallego JM, Alcamí M, Klyatskaya S, Ruben M, Martín F, Miranda R, Ecija D, Barth JV. Surface-supported robust 2D lanthanide-carboxylate coordination networks. Small 2015;11:6358–64. https://doi.org/10.1002/smll.201502761.

[36] Lepnev LS, Vashchenko AA, Vitukhnovskii AG, Eliseeva SV, Kotova OV, Kuzmina NP. Degradation of organic light-emitting diodes based on different-ligand complexes of terbium (III) salicylate and 2-phenoxybenzoate. Bull Lebedev Phys Inst 2007;34:102–6. https://doi.org/10.3103/S1068335607040021.

[37] Utochnikova V, Kalyakina A, Kuzmina N. New approach to deposition of thin luminescent films of lanthanide aromatic carboxylates. Inorg Chem Commun 2012;16:4–7. https://doi.org/10.1016/j.inoche.2011.11.009.

[38] Utochnikova VV, Pietraszkiewicz O, Koźbiał M, Gierycz P, Pietraszkiewicz M, Kuzmina NP, Kózbial M, Gierycz P, Pietraszkiewicz M, Kuzmina NP. Mixed-ligand terbium terephthalates: synthesis, photophysical and thermal properties and use

for luminescent terbium terephthalate thin film deposition. J Photochem Photobiol A Chem 2013;253:72–80. https://doi.org/10.1016/j.jphotochem.2012.12.021.
[39] Aslandukov AN, Utochnikova VV, Goriachiy DO, Vashchenko AA, Tsymbarenko DM, Hoffmann M, Pietraszkiewicz M, Kuzmina NP, Information ES. The development of a new approach toward lanthanide-based OLED fabrication: new host materials for Tb-based emitters. Dalton Trans 2018;47:16350–7. https://doi.org/10.1039/C8DT02911C.
[40] Kalyakina AS, Utochnikova VV, Sokolova EY, Vaschenko AA, Lepnev LS, Van Deun R, Trigub ALAL, Zubavichus YVYV, Hoffmann M, Mühl S, Kuzmina NP, Vashchenko AA, Lepnev LS, Van Deun R, Trigub AL, Zubavichus YV, Hoffmann M, Mühl S, Kuzmina NP. OLED thin film fabrication from poorly soluble terbium o-phenoxybenzoate through soluble mixed-ligand complexes. Org. Electron. Physics, Mater. Appl. 2016;28:319–29https://doi.org/10.1016/j.orgel.2015.11.006.
[41] Yao Y, Zhang Y, Shen Q, Yu K. Synthesis, reactivity, and structure of mixed-ligand ytterbium complexes supported by β-diketiminate. Organometallics 2002;21:819–24. https://doi.org/10.1021/om010803a.
[42] Ram C, Sivamani S, Micha Premkumar T, Hariram V. Computational study of leading edge jet impingement cooling with a conical converging hole for blade cooling. ARPN J. Eng. Appl. Sci. 2017;12:6397–406. https://doi.org/10.1039/b000000x.
[43] D'Aléo A, Picot A, Baldeck PL, Andraud C, Maury O. Design of dipicolinic acid ligands for the two-photon sensitized luminescence of europium complexes with optimized cross-sections. Inorg Chem 2008;47:10269–79. https://doi.org/10.1021/ic8012975.
[44] D'Aléo A, Picot A, Beeby A, Williams JAG, Leguennic B, Andraud C, Maury O. Efficient sensitization process of europium, ytterbium and neodymium through charge-transfer excited state. Inorg Chem 2008;47:10258.
[45] V Eliseeva S, Auböck G, Van Mourik F, Cannizzo A, Song B, Deiters E, Chauvin A, Chergui M, Bünzli JG. Multiphoton-excited luminescent lanthanide bioprobes : two- and three-photon cross sections of dipicolinates derivatives and binuclear helicates Laboratory of Lanthanide Supramolecular Chemistry. Lausanne: Swiss Federal Institute of Technology; 2010. p. 5–11. S1 S2.
[46] Law GL, Wong KL, Man CWY, Wong WT, Tsao SW, Lam MHW, Lam PKS. Emissive terbium probe for multiphoton in vitro cell imaging. J Am Chem Soc 2008;130:3714–5. https://doi.org/10.1021/ja710418d.
[47] Belousov YA, Utochnikova VV, Kuznetsov SS, Andreev MN, Dolzhenko VD, Drozdov AA. New rare-earth metal acyl pyrazolonates: synthesis, crystals structures, and luminescence properties. Russ J Coord Chem 2014;40:627–33. https://doi.org/10.1134/S1070328414090024.
[48] Bünzli J-CG. On the design of highly luminescent lanthanide complexes. Coord Chem Rev 2015;293–294:19–47. https://doi.org/10.1016/j.ccr.2014.10.013.
[49] Clarkson I, Dickins R, de Sousa A, others. Non-radiative deactivation of the excited states of europium, terbium and ytterbium complexes by proximate energy-matched OH, NH and CH oscillators: an improved luminescence method for establishing solution hydration states. J. Chem. Soc. Perkin Trans. 1999;2:493–504.
[50] Lis S, Hnatejko Z, Barczynski P, Elbanowski M. Luminescence studies of Eu(III) mixed ligand complexes. J Alloy Comp 2002;344:70–4. https://doi.org/10.1016/S0925-8388(02)00310-9.
[51] Utochnikova VV, Solodukhin NN, Aslandukov AA, Zaitsev KV, Kalyakina AS, Averin AA, Ananyev IA, Churakov AV, Kuzmina NP. Highly luminescent, water-soluble lanthanide fluorobenzoates: syntheses, structures and photophysics. Part II: luminescence enhancement by p-substituent variation. Eur J Inorg Chem 2016:107–14https://doi.org/10.1002/ejic.201600843.
[52] Hänninen P, Härmä H, editors. Lanthanide luminescence Berlin, Heidelberg: Springer Berlin Heidelberg; 2011. https://doi.org/10.1007/978-3-642-21023-5.
[53] Zheng Y, Lin J, Liang Y, Yu Y, Zhou Y, Guo C, Wang S, Zhang H. A novel way to enhance electroluminescence performance based on soluble binary and ternary europium 1,1,1-trifluoroacetylacetonate complexes. J Alloy Comp 2002;336:114–8. https://doi.org/10.1016/S0925-8388(01)01887-4.
[54] Lin Y, Wal CM. Supercritical fluid extraction of lanthanides with fluorinated [beta]-Diketones and tributyl phosphate. 2000. 2000.
[55] Utochnikova VV, Latipov EV, Dalinger AI, Nelyubina YV, Vashchenko AA, Hoffmann M, Kalyakina AS, Vatsadze SZ, Schepers U, Bräse S, Kuzmina NP. Lanthanide pyrazolecarboxylates for OLEDs and bioimaging. J Lumin 2018;202:38–46. https://doi.org/10.1016/j.jlumin.2018.05.022.
[56] Novikov SV, Vannikov AV. Charge induced energy fluctuations in thin organic films: effect on charge transport. Synth Met 2001;121:1387–8. https://doi.org/10.1016/S0379-6779(00)00994-2.
[57] Yu X, Su Q. Photoacoustic and luminescence properties study on energy transfer and relaxation processes of Tb(III) complexes with benzoic acid. J Photochem Photobiol A Chem 2003;155:73–8. https://doi.org/10.1016/S1010-6030(02)00362-3.
[58] Hilder M, Lezhnina M, Junk PC, Kynast UH. Spectroscopic properties of lanthanoid benzene carboxylates in the solid state: Part 3. N-heteroaromatic benzoates and 2-furanates. Polyhedron 2013;52:804–9. https://doi.org/10.1016/j.poly.2012.07.047.
[59] Bünzli J-CG. Review: lanthanide coordination chemistry: from old concepts to coordination polymers. J Coord Chem 2014;67:3706–33. https://doi.org/10.1080/00958972.2014.957201.
[60] Utochnikova VV, Abramovich MS, Latipov EV, Dalinger AI, Goloveshkin AS, Vashchenko AA, Kalyakina AS, Vatsadze SZ, Schepers U, Bräse S, Kuzmina NP. Brightly luminescent lanthanide pyrazolecarboxylates: synthesis, luminescent properties and influence of ligand isomerism. J Lumin 2019;205:429–39. https://doi.org/10.1016/J.JLUMIN.2018.09.027.
[61] Kalsi PSS, K.S.P., Kalsi PSS. Spectroscopy of organic compounds. sixth ed. Delhi: New Age International; 2004.
[62] Kusrini E, Adnan R, Saleh MI, Yan L-K, Fun H-K. Synthesis and structure of dimeric anthracene-9-carboxylato bridged dinuclear erbium(III) complex, [Er2(9-AC)6(DMF)2(H2O)2]. Spectrochim Acta Part A Mol Biomol Spectrosc 2009;72:884–9. https://doi.org/10.1016/j.saa.2008.12.011.
[63] Shuvaev S, Utochnikova V, Marciniak L, Freidzon A, Sinev I, Van Deun R, Freire RO, Zubavichus Y, Gruenert W, Kuzmina N, Shuvaev S, Utochnikova V, Marciniak Ł, Freidzon A, Sinev I, Van Deun R, Freire RO, Zubavichus Y, Grunert W, Kuzmina N. Lanthanide complexes with aromatic o-phosphorylated ligands: synthesis, structure elucidation and photophysical properties. Dalton Trans 2014;43:3121–36. https://doi.org/10.1039/c3dt52600c.
[64] Utochnikova VV, Kovalenko AD, Burlov AS, Marciniak L, Ananyev IV, Kalyakina AS, Kurchavov NA, Kuzmina NP. Lanthanide complexes with 2-(tosylamino)benzylidene-N-benzoylhydrazone, which exhibit high NIR emission. Dalton Trans 2015;44:12660–9. https://doi.org/10.1039/C5DT01161B.
[65] Utochnikova VV, Kuzmina NP. Photoluminescence of lanthanide aromatic carboxylates. Russ J Coord Chem 2016;42:679–94. https://doi.org/10.1134/S1070328416090074.
[66] Ferenc W, Walkow-Dziewulska A. Complexes of heavy lanthanides and yttrium with 3,4-dimethoxybenzoic acid. J Therm Anal Calorim 2000;61:923–33. https://doi.org/10.1023/A:1010111011794.
[67] Zhuravlev KP, Tsaryuk VI, Pekareva IS, Sokolnicki J, Klemenkova ZS. Europium and terbium ortho-, meta-, and para-methoxybenzoates: structural peculiarities, luminescence, and energy transfer. J Photochem Photobiol A Chem 2011;219:139–47. https://doi.org/10.1016/j.jphotochem.2011.02.003.
[68] Tsaryuk VI, Zhuravlev KP, Vologzhanina AV, Kudryashova V a, Zolin VF. Structural regularities and luminescence properties of dimeric europium and terbium carboxylates with 1,10-phenanthroline (C.N. = 9). J Photochem Photobiol A Chem 2010;211:7–19. https://doi.org/10.1016/j.jphotochem.2010.01.012.
[69] Arnaud N, Georges J. Comprehensive study of the luminescent properties and lifetimes of Eu3+ and Tb3+ chelated with various ligands in aqueous solutions: influence of the synergic agent, the surfactant and the energy level of the ligand triplet. Spectrochim Acta Part A Mol Biomol Spectrosc 2003;59:1829–40. https://doi.org/10.1016/S1386-1425(02)00414-6.
[70] Hilder M, Lezhnina MM, Junk PC, Kynast UH, Lezhnina MM. Spectroscopic properties of lanthanoid benzene carboxylates in the solid state: Part 1. J Photochem Photobiol A Chem 2009;202:10–20. https://doi.org/10.1016/j.jphotochem.2008.10.026.
[71] Koner R, Goldberg I. A unique two-dimensional coordi-nation network of 1-benzofuran-2,3-di-car- boxyl-ate with lanthanum(III) obtained by solvothermal synthesis. Acta Crystallogr Sect C Cryst Struct Commun 2009;65:149–51. https://doi.org/10.1107/S0108270109007161.
[72] Utochnikova VV, Koshelev DS, Medvedko AV, Kalyakina AS, Bushmarinov IS, Grishko AY, Schepers U, Bräse S, Vatsadze SZ. Europium 2-benzofuranoate: synthesis and use for bioimaging. Opt. Mater. (Amst). under revi 2017:191–6. https://doi.org/10.1016/j.optmat.2017.05.038.
[73] Trivedi ER, Eliseeva SV, Jankolovits J, Olmstead MM, Petoud S, Pecoraro VL. Highly emitting near-infrared lanthanide "encapsulated sandwich" metallacrown complexes with excitation shifted toward lower energy. J Am Chem Soc 2014;136:1526–34. https://doi.org/10.1021/ja4113337.
[74] Ning G, Lu X, Gong W, Ye J, Gao H, Wang Q, Lin Y. Effect of auxiliary-ligand on assembly of lanthanide(III) complexes with quinoline-2-carboxylic acid: synthesis, structure, photoluminescent and magnetic properties. Inorg Chim Acta 2011;384:1–7. https://doi.org/10.1016/j.ica.2011.11.028.
[75] Xu W, Zhou Y, Huang D, Xiong W, Su M, Wang K, Han S, Hong M. Crystal structure, multiplex photoluminescence, and magnetic properties of a series of lanthanide coordination polymers based on quinoline carboxylate ligand. Cryst Growth Des 2013;13:5420–32. https://doi.org/10.1021/cg401391b.
[76] Zhang H, Fan R, Wang P, Wang X, Gao S, Dong Y, Wang Y, Yang Y. Structure variations of a series of lanthanide complexes constructed from quinoline carboxylate ligands: photoluminescent properties and PMMA matrix doping. RSC Adv 2015;5:38254–63. https://doi.org/10.1039/C5RA01796C.
[77] Bünzli JCG, Chauvin AS, Kim HK, Deiters E, Eliseeva SV. Lanthanide luminescence efficiency in eight- and nine-coordinate complexes: role of the radiative lifetime, Coord. Chem Rev 2010;254:2623–33. https://doi.org/10.1016/j.ccr.2010.04.002.
[78] Bünzli JCG, Comby S, Chauvin AS, Vandevyver CDB. New opportunities for lanthanide luminescence. J Rare Earths 2007;25:257–74. https://doi.org/10.1016/S1002-0721(07)60420-7.
[79] Khudoleeva VY, Utochnikova VV, Kalyakina AS, Deygen IM, Shiryaev AA, Marciniak Ł, Lebedev VA, Roslyakov IV, Garshev AV, Lepnev LS, Schepers U, Bräse S, Kuzmina NP. Surface modified EuxLa1-xF3 nanoparticles as luminescent biomarkers: still plenty of room at the bottom. Dyes Pigments 2017;143:348–55. https://doi.org/10.1016/j.dyepig.2017.04.058.
[80] Dolomanov OV, Bourhis LJ, Gildea RJ, Howard JAK, Puschmann H. OLEX2: a complete structure solution, refinement and analysis program. J Appl Crystallogr 2009;42:339–41. https://doi.org/10.1107/S0021889808042726.
[81] Bourhis LJ, Dolomanov OV, Gildea RJ, Howard JAK, Puschmann H. The anatomy of a comprehensive constrained, restrained refinement program for the modern computing environment - olex2 dissected. Acta Crystallogr. Sect. A Found. Crystallogr. 2015;71:59–75. https://doi.org/10.1107/S2053273314022207.
[82] Sheldrick GM. Crystal structure refinement with SHELXL. Acta Crystallogr. Sect. C Struct. Chem. 2015;71:3–8. https://doi.org/10.1107/S2053229614024218.
[83] A.A. Granovsky, Firefly version 8., (n.d.).
[84] Stuttgart, Cologne, Stuttgart/Cologne energy-consistent (ab initio) pseudopotentials, (n.d.).
[85] Vechorkin O, Hirt N, Hu X. Carbon dioxide as the C1 source for direct C-H functionalization of aromatic heterocycles. Org Lett 2010;12:3567–9. https://doi.org/

10.1021/ol101450u.
[86] Kamps JJAG, Belle R, Mecinović J. Hydroxylamine as an oxygen nucleophile: substitution of sulfonamide by a hydroxyl group in benzothiazole-2-sulfonamides. Org Biomol Chem 2013;11:1103–8. https://doi.org/10.1039/C2OB26929E.
[87] Boogaerts IIF, Nolan SP. Carboxylation of C-H bonds using N -heterocyclic carbene gold(I) complexes. J Am Chem Soc 2010;132:8858–9. https://doi.org/10.1021/ja103429q.
[88] Musser JH, Hudec TT, Bailey K. A simple one-step synthesis of alkyl benzazol-2-carboxylates. Synth Commun 1984;14:947–53. https://doi.org/10.1080/00397918408063765.
[89] Zavarzin IV, Yarovenko VN, Chernoburova EI, Krayushkin MM, Edition I. Synthesis of monothiooxamides. Russ Chem Bull 2004;53:476–7. https://doi.org/10.1023/B:RUCB.0000030819.80699.6e.
[90] Suzuki N, Goto T. Synthesis of 4-thiazolone derivatives related to firefly oxyluciferin. Agric Biol Chem 1972;36:2213–21. https://doi.org/10.1080/00021369.1972.10860525.
[91] Bleaney B. Nuclear magnetic resonance shifts in solution due to lanthanide ions. J Magn Reson 1972;8:91–100. https://doi.org/10.1016/0022-2364(72)90027-3.
[92] Friebolin H, Becconsall JK. Basic one-and two-dimensional NMR spectroscopy. VCH Weinheim; 1993.
[93] Corsi DM, Platas-Iglesias C, van Bekkum H, Peters JA. Determination of paramagnetic lanthanide (III) concentrations from bulk magnetic susceptibility shifts in NMR spectra. Magn Reson Chem 2001;39:723–6.
[94] Utochnikova VV, Solodukhin NN, Aslandukov AA, Zaitsev KV, Kalyakina AS, Averin AA, Ananyev IA, Churakov AV, Kuzmina NP. Luminescence enhancement by p -substituent variation. Eur J Inorg Chem 2017;2017:107–14. https://doi.org/10.1002/ejic.201600843.
[95] Brzyska W, Kula A. Studies on the thermal decomposition of rare earth element complexes with 2-haphtoic acid. Thermodyn. Acta. 1995;44:1159–69.
[96] Bünzli JCG. Lanthanide luminescence for biomedical analyses and imaging. Chem Rev 2010;110:2729–55. https://doi.org/10.1021/cr900362e.
[97] Latva M, Takalo H, Mukkala V-M, Matachescu C, Rodríguez-Ubis JC, Kankare J. Correlation between the lowest triplet state energy level of the ligand and lanthanide(III) luminescence quantum yield. J Lumin 1997;75:149–69. https://doi.org/10.1016/S0022-2313(97)00113-0.
[98] Monteiro JHSK, Formiga ALB, Sigoli FA. The influence of carboxilate, phosphinate and seleninate groups on luminescent properties of lanthanides complexes. J Lumin 2014;154:22–31. https://doi.org/10.1016/j.jlumin.2014.03.071.
[99] Solodukhin NN, Utochnikova VV, Lepnev LS, Kuzmina NP. Mixed-ligand terbium hydroxyaromatic carboxylates with o-phenanthroline: luminescence quenching at 300 and 77K. Mendeleev Commun 2014;24:91–3. https://doi.org/10.1016/j.mencom.2014.03.008.
[100] Varaksina EA, Taydakov IV, Ambrozevich SA, Selyukov AS, Lyssenko KA, Jesus LT, Freire RO. Influence of fluorinated chain length on luminescent properties of Eu3+β-diketonate complexes. J Lumin 2018;196:161–8. https://doi.org/10.1016/j.jlumin.2017.12.006.
[101] Stein G. Energy gap law in the solvent isotope effect on radiationless transitions of rare earth ions. J Chem Phys 1975;62:208. https://doi.org/10.1063/1.430264.
[102] Chesnokov GA, Topchiy MA, Asachenko AF, Muravyev NV, Grishin LI, Nikiforova AS, Utochnikova VV, Rybakov VB, Khrustalev VN, Nechaev MS. No title. Eur J Inorg Chem 2018;2018:805–15. https://doi.org/10.1002/ejic.201701154.
[103] Piemontese L, Carbonara G, Fracchiolla G, Laghezza A, Tortorella P, Loiodice F. Convenient synthesis of some 3-phenyl-1-benzofuran-2-carboxylic acid derivatives as new potential inhibitors of ClC-Kb channels. Heterocycles 2010;81:2865–72. https://doi.org/10.3987/COM-10-12070.
[104] Cui Y, Zhu F, Chen B, Qian G. Metal–organic frameworks for luminescence thermometry. Chem Commun 2015;51:7420–31. https://doi.org/10.1039/C5CC00718F.
[105] Brites CDS, Millán A, Carlos LD. Lanthanides in luminescent thermometry. Handb. Phys. Chem. Rare earths 2016. p. 339–427. https://doi.org/10.1016/bs.hpcre.2016.03.005.
[106] Kovalenko A, Rublev PO, Tcelykh LO, Goloveshkin AS, Lepnev LS, Burlov AS, Vashchenko AA, Marciniak L, Magerramov AM, Shikhaliyev NG, Vatsadze SZ, Utochnikova VV. Lanthanide complexes with 2-(tosylamino)-benzylidene-N-(aryloyl)hydrazones - universal luminescent materials. Chem Mater 2019. https://doi.org/10.1021/acs.chemmater.8b03675. acs.chemmater.8b03675.
[107] Khudoleeva V, Tcelykh L, Kovalenko A, Kalyakina A, Goloveshkin A, Lepnev L, Utochnikova V. Terbium-europium fluorides surface modified with benzoate and terephthalate anions for temperature sensing: does sensitivity depend on the ligand? J Lumin 2018;201:500–8. https://doi.org/10.1016/j.jlumin.2018.05.002.
[108] Ferenc W, Walków-Dziewulska A. Thermal and spectral properties of 2,3-, 2,4- and 3,4- dimethoxybenzoates of light lanthanides. J Therm Anal Calorim 2002;70:949–58. https://doi.org/10.1023/A:1022280909229.
[109] Petoud Stéphane, Cohen Seth M, Bünzli Jean-Claude G, Raymond † Kenneth N. Stable lanthanide luminescence agents highly emissive in aqueous Solution: multidentate 2-hydroxyisophthalamide complexes of Sm3+, Eu3+, Tb3+, Dy3+. 2003. https://doi.org/10.1021/JA0379363.
[110] Kim T-Y, Jung J-H, Kim J-B, Moon D-G. Achieving high efficiency by high temperature annealing of hole transporting polymer layer in solution-processed organic light-emitting devices. Synth Met 2017;232:167–70. https://doi.org/10.1016/j.synthmet.2017.08.004.
[111] Thejo Kalyani N, Dhoble SJ. Organic light emitting diodes: energy saving lighting technology—a review. Renew Sustain Energy Rev 2012;16:2696–723. https://doi.org/10.1016/j.rser.2012.02.021.
[112] Gaynor W, Hofmann S, Christoforo MG, Sachse C, Mehra S, Salleo A, McGehee MD, Gather MC, Lüssem B, Müller-Meskamp L, Peumans P, Leo K. Color in the corners: ITO-free white OLEDs with angular color stability. Adv Mater 2013;25:4006–13. https://doi.org/10.1002/adma.201300923.
[113] Weiss CJ, Marks TJ. Organo-f-element catalysts for efficient and highly selective hydroalkoxylation and hydrothiolation. Dalton Trans 2010;39:6576. https://doi.org/10.1039/c003089a.